available at www.sciencedirect.com

ScienceDirect

www.elsevier.com/locate/brainres

BRAIN RESEARCH

Research Report

Neural circuitry for accurate identification of facial emotions

James Loughead[a,*], Ruben C. Gur[a,b], Mark Elliott[b], Raquel E. Gur[a,b]

[a]Department of Psychiatry, University of Pennsylvania, Philadelphia, PA 19104, USA
[b]Department of Radiology, University of Pennsylvania, Philadelphia, PA 19104, USA

ARTICLE INFO

Article history:
Accepted 31 October 2007
Available online 17 November 2007

Keywords:
Emotion
Amygdala
fMRI
Affect
Mixed design
Limbic

ABSTRACT

Converging studies have revealed neural circuits for emotion processing, yet none has related activation to identification accuracy. We report a hybrid (block and event-related) fMRI study in 17 healthy adults, which permitted performance-based analysis. As in earlier studies, blocked analysis of the facial emotion identification task showed activation of amygdala, fusiform, thalamus, inferior and midfrontal regions. However, an event-related analysis of target stimuli demonstrated time locked activation associated with correct identification of happy, sad, angry and fearful faces. Overall, correct detection of angry and fearful faces was associated with greater activation compared to incorrect responses, especially in the amygdala and fusiform gyrus. The opposite was observed for happy and sad faces, where greater thalamic and midfrontal activation portended incorrect responses. Results indicate that the fusiform cortex and amygdala respond differentially in the four target conditions (happy, sad, angry and fearful) along the dimension of threat-relatedness.

1. Introduction

Brain systems for modulating emotions are being elucidated with complementary animal paradigms (LeDoux, 2000, 2003), studies in patients with brain lesions (Adolphs et al., 2005; Damasio, 1997) and functional neuroimaging experiments in healthy people (Morris and Dolan, 2004; Phelps, 2004; Phelps et al., 2004; Vuilleumier, 2005; Vuilleumier et al., 2003; Whalen et al., 2004). Converging findings have identified the major components of a neural network involving interactions among amygdala and other limbic regions, thalamus and sensory cortex, and prefrontal regions (Morris et al., 1998).

Meta-analyses of fMRI experiments support a fear-specific response of the amygdala (Phan et al., 2002). The focus on fear stems from the rich literature on fear conditioning in rodents, with paradigms that can be translated to human fMRI studies (Baas et al., 2004; Buchel et al., 1998; Knight et al., 1999; LaBar et al., 1998; Morris and Dolan, 2004; Murphy et al., 2003; Phan et al., 2002). Fewer investigations have examined neural systems involved in the identification of a range of human emotional displays, an important ability in social settings. Because the face predominates in conveying emotion within and across species (Darwin, 1872), studies examining affect identification have used primarily facial stimuli. Strong evidence for amygdala activation in response to faces expressing fear (Hariri et al., 2003; Morris et al., 1996; Phillips et al., 1997; Whalen et al., 2001) and anger (Whalen et al., 2001) has accumulated. Involvement of the amygdala in processing other emotions such as happiness and sadness has also been suggested (Britton et al., 2006; Fitzgerald et al., 2006; Schneider et al., 1997), but remains less thoroughly investigated.

Using a blocked-design fMRI study, we have previously reported greater amygdala, thalamus and inferior frontal activation when facial expressions were relevant (identification of emotional valence), compared to a condition where affective judgment was not required (age determination) (Gur et al.,

* *Corresponding author*. University Of Pennsylvania, 3400 Spruce Street, Gates Building, 10th Floor, Philadelphia, PA 19107, USA. Fax: +1 215 662 7903.
E-mail address: loughead@bbl.med.upenn.edu (J. Loughead).

0006-8993/$ – see front matter © 2007 Elsevier B.V. All rights reserved.
doi:10.1016/j.brainres.2007.10.105

2002a,b). However, all emotions were grouped (blocked) and the task required assigning positive or negative valence to the expressed emotion, rather than identifying individual emotions (happy, sad, angry, and fearful). No study has yet compared the response to each of these four universal emotions, nor tested whether activation differs for correctly detected emotions compared to incorrect responses.

We addressed these questions with a hybrid (blocked and event-related) fMRI experiment at high-field (4 Tesla), in which we measured cerebral activity using blood oxygenation level dependent (BOLD) contrast during a facial emotion identification task. The block feature permitted comparative assessment of activation for the task of identifying happy, sad, angry and fearful expressions. Event-related analyses isolated activation time-locked to the presentation of a specific expression relative to neutral faces and, importantly, separated activation for correct and incorrect responses. This analysis revealed a network of regions that differentially signaled the four target emotions, principally along the dimension of threat-relatedness, yielding a unique "signature" for the accurate identification of each.

2. Results

2.1. Task performance

The response rate (97% overall) did not differ among the four target emotions [F (3, 14) = 0.99, $p = 0.427$] indicating that participants remained attentive throughout the lengthy scanning session. As expected, participants identified happy facial expressions with the greatest accuracy [F (3, 14) = 15.27, $p < 0.005$] and speed [F (3, 14) = 10.90, $p < 0.005$] compared to all other emotions (Table 1).

Table 1 – Performance during emotion identification task by stimuli class

Performance measure	Mean	S.D.	Min	Max
Percent Total Correct (TC) N = 17				
Happy	95.97	5.21	73.33	98.33
Sad	84.21	18.41	35.00	92.50
Anger	86.08	10.54	47.50	94.17
Fear	82.42	12.11	41.67	89.17
Reaction time TC (ms) N = 17				
Happy	890	133	631	1089
Sad	949	181	540	1289
Anger	1020	152	707	1201
Fear	983	202	740	1371
Target Correct (max 32) N = 17				
Happy	28.12	3.87	20	30
Sad	21.82	7.80	10	30
Anger	18.12	5.74	11	27
Fear	18.94	5.02	9	25
Target Correct[1] *(max 32) N = 14*				
Happy	27.93	3.22	20	29
Sad	22.93	6.94	10	27
Anger	19.43	4.80	11	26
Fear	19.00	4.00	11	25

[1] Subset of the sample created by trimming the upper and lower quartile for Target Correct across all emotion.

2.2. Block analysis

The block analysis (Table 2, left half, and Fig. 1a) showed significant activation for the emotion identification task in a distributed network of regions that included clusters in bilateral frontal, amygdala, thalamus, fusiform gyrus and cuneus regions as well as right parahippocampal and angular gyri, and cerebellum. Consistent with previous studies, these regions showed robust activation across all four target emotions, and appear to sustain emotion identification of facial stimuli (Britton et al., 2006; Fitzgerald et al., 2006; Gur et al., 2002a,b). The only region to show differential activation among the four emotions was the inferior frontal gyrus (Fig. 1a, blue region), an effect driven by this region's failure to activate during Happy target blocks (Fig. 1b).

2.3. Event-related analysis

The event-related analysis examined signal change that was time-locked to the appearance of a specific emotion and separated correct from incorrect identifications. Five regions showed significant differences by emotion, correct versus incorrect, or an interaction of these factors (Table 1, right half, and Fig. 2a). To identify the source of the main effects and interactions, we extracted the percent signal change values from these regions bilaterally (fusiform gyrus, thalamus, amygdala, inferior frontal gyrus and middle frontal gyrus) for further analysis.

As can be seen in Fig. 2b, the recruited regions differed in their response depending on the displayed emotion and whether it was correctly identified. All emotional faces activated thalamus, amygdala and inferior frontal regions more than neutral faces, but each emotion had a unique "signature" differentiating correct from incorrect identifications. For threat-related target expressions (anger and fear), correct identifications were associated with greater activation than incorrect identifications. This association was seen specifically in the amygdala for anger and in all identified regions for fear. By contrast, for the non-threat-related expressions of happiness and sadness, error was associated with greater activation, especially of the thalamus for happiness and midfrontal regions for sadness.

To explore the consequence that performing at ceiling (or floor) levels may have on the estimated magnitude of brain response, we created a subgroup by trimming the upper and lower quartile for Target Correct performance (Table 1, last rows). This eliminated three subjects: 1) one who had performed very well on Happy targets (30/32) and Anger targets (27/32); 2) one who had performed poorly on Sad targets (9/32) and 3) one who performed very well on sad targets (30/32). This subgroup was submitted to the same analysis described above and showed a virtually identical pattern of activation compared to the full sample (Fig. 3). Similarly, the plot of percent signal change from these regions was remarkably unchanged (not shown).

Table 2 – Cluster location and local maxima of BOLD signal change for block and event bases analyses

#	Cluster label and subregions	HEM	Task-based activation common to all target emotions (Happy, Sad, Angry, Fearful) Count	Local maxima Max Z	x	y	z	Event-based accuracy main effect Count	Local maxima Max Z	x	y	z	Event-based emotion main effect Count	Local maxima Max Z	x	y	z	Accuracy by emotion interaction Count	Local maxima Max Z	x	y	z
1	Right inferior frontal		2938		47	17	9															
	Inferior frontal gyrus	R	2028	6.09	48	27	−3	58	1.99	40	32	−6	785	3.59	46	25	−10	57	1.97	48	2	28
	Precentral gyrus	R	423	5.45	42	−2	30															
	Insula	R	226	5.73	42	7	18															
	Superior temporal gyrus	R	100	5.69	46	19	−11															
	Middle frontal gyrus	R	59	5.13	53	17	27															
2	Right inferior frontal		48		46	55	0															
	Middle frontal gyrus	R	21	4.62	46	52	−1															
	Inferior frontal gyrus	R	27	4.68	46	52	1															
3	Left inferior frontal		748		−36	19	−3															
	Inferior frontal gyrus	L	269	5.35	−44	17	−4	34	2.47	−30	34	−14	466	2.93	−36	23	−11	267	2.46	−30	25	4
	Insula	L	68	5.08	−30	20	10															
	Claustrum	L	62	5.42	−28	20	12															
	Superior temporal gyrus	L	36	5.05	−42	15	−14															
	Putamen lentiform nucleus	L	33	4.83	−22	19	−4															
4	Left inferior frontal		157		−37	8	26															
	Precentral gyrus	L	40	5.05	−38	3	27															
	Middle frontal gyrus	L	22	4.75	−40	13	25											26	2.1	−44	10	27
	Inferior frontal gyrus	L	85	5.09	−38	5	27															
5	Right amygdala		239		22	−10	−20															
	Right parahippocampal gyrus	R	138	5.16	24	−13	−21															
	Amygdala	R	101	5.34	20	−8	−20	97	3.41	24	−5	−22						89	2.91	14	−12	−18
6	Left amygdala		924		−11	−19	−15															
	Parahippocampal gyrus	L	399	5.08	−12	−11	−21															
	Culmen	L	271	4.83	−6	−28	−15															
	Amygdala	L	178	4.52	−16	−6	−11	26	2.4	−20	−8	−18										
	Red nucleus	L	69	4.78	0	−26	−17															
	Substantia nigra	L	67	4.78	−10	−22	−11															
	Hippocampus	L	42	4.75	−30	−13	−18															
7	Right thalamus		195		15	−9	−14															
	Thalamus	R	159	5.23	12	−7	13						15	2.24	8	−8	8	122	3.74	8	−8	8
	Caudate	R	38	4.91	12	−5	17															
8	Left thalamus		591		−10	−14	11															
	Thalamus	L	577	4.69	−10	−17	5	11	1.84	−6	−12	8						424	3.96	−2	−22	10
9	Right fusiform gyrus		315		43	−77	−9															
	Fusiform gyrus	R	100	5.22	36	−80	−11						19	2.25	46	−55	−16					
	Middle occipital gyrus	R	76	4.82	50	−76	−6															
	Inferior occipital gyrus	R	77	5.27	38	−80	−11															
10	Right fusiform gyrus		98		44	−51	−19															
	Fusiform gyrus	R	98	4.97	42	−56	−20															

(continued on next page)

Table 2 (*continued*)

#	Cluster label and subregions	HEM	Task-based activation common to all target emotions (Happy, Sad, Angry, Fearful)					Event-based accuracy main effect					Event-based emotion main effect					Accuracy by emotion interaction				
			Count	Local maxima				Count	Local maxima				Count	Local maxima				Count	Local maxima			
				Max Z	x	y	z		Max Z	x	y	z		Max Z	x	y	z		Max Z	x	y	z
11	Left fusiform gyrus		432		−43	−69	−14															
	Fusiform gyrus	L	294	5.4	−44	−59	−19											21	2.17	−46	−62	−16
	Inferior occipital gyrus	L	146	5.67	−46	−82	−13															
	Middle occipital gyrus	L	21	4.81	−44	−76	−10															
12	Right parahippocampal gyrus		269		33	−34	−6															
	Parahippocampa gyrus	R	121	4.97	32	−35	−3															
	Hippocampus	R	54	5.04	30	−35	−9															
	Fusiform gyrus	R	30	4.98	40	−41	−7															
13	Right cuneus		186		25	−97	0															
	Middle occipital gyrus	R	53	5.16	28	−99	2															
	Lingual gyrus	R	34	5.32	22	−99	−3															
	Cuneus	R	87	5.36	20	−101	−3															
14	Left cuneus		67		−19	−100	−2															
	Lingual gyrus	L	20	4.57	−18	−99	−5															
	Cuneus	L	41	4.77	−18	−101	−5															
15	Right angular gyrus		64		36	−55	33															
	Angular gyrus	R	64	4.91	36	−55	34															
16	Right cerebellum		140		2	−55	19															
	Cerebellum	R	140	5.03	2	−57	19															

3. Discussion

As in earlier studies that used blocked analyses, we found a network of regions activated during the top-down emotion identification task, which prominently included fusiform gyrus, amygdala, thalamus and prefrontal regions. These regions have been implicated in earlier studies (Britton et al., 2006; Gur et al., 2002a,b) and support the sensory, evaluative, attentional and mnemonic requirements of the task.

The new findings relate to effects of bottom-up activation by a target emotion, which differed by displayed emotion and accuracy of identification. For angry and fearful faces, correct identification was associated with greater activation than incorrect responses. The effect was seen for the fusiform gyrus and amygdala in response to both anger and fear, and also in the thalamus and frontal regions in response to fearful faces. In contrast, for happiness and sadness–expressions that are not threat-related–correct identification occurred when there was less activation than for incorrect responses. For Happy, there was less thalamic activation for correct than for incorrect responses, while for Sad, correct responding occurred with relatively reduced middle frontal activation. Thus it appears that fusiform and amygdala activation is necessary for correct identification of threat-related expressions and errors occur when these regions fail to activate. For non-threat-related expressions, errors occur with excessive activation of thalamocortical circuits. This suggests that while the amygdala is generally involved in the processing of universal emotional expressions, it has a special role in the accurate identification of expressions that convey an imminent threat to survival.

Several limitations of this study are noteworthy. The task was simplified to minimize response confusion (binary choice) at the expense of some ecological validity when compared to open ended or multiple choice response formats. Another limitation is the use of an active baseline (neutral faces) for the event-related analysis. This design provides the most rigorous contrast for demonstrating the additive effect of emotional content controlling for other aspects of face processing, but it precludes separate modeling of response to neutral expressions. These limitations notwithstanding, our study has identified a neural system that is necessary for correct identification of facial emotions, in which signaling occurs by both increased and decreased regional activation. Future studies could further isolate activations resulting in specific types of misidentifications and evaluate whether disturbances in this system can explain social behavioral deficits associated with neuropsychiatric disorders.

4. Experimental procedures

4.1. *Subjects*

We studied 17 (11 men, 6 women) healthy right-handed participants age 22–34 years (mean = 26.94, S.D. = 3.49). After complete description of the study to the subjects, written informed consent was obtained.

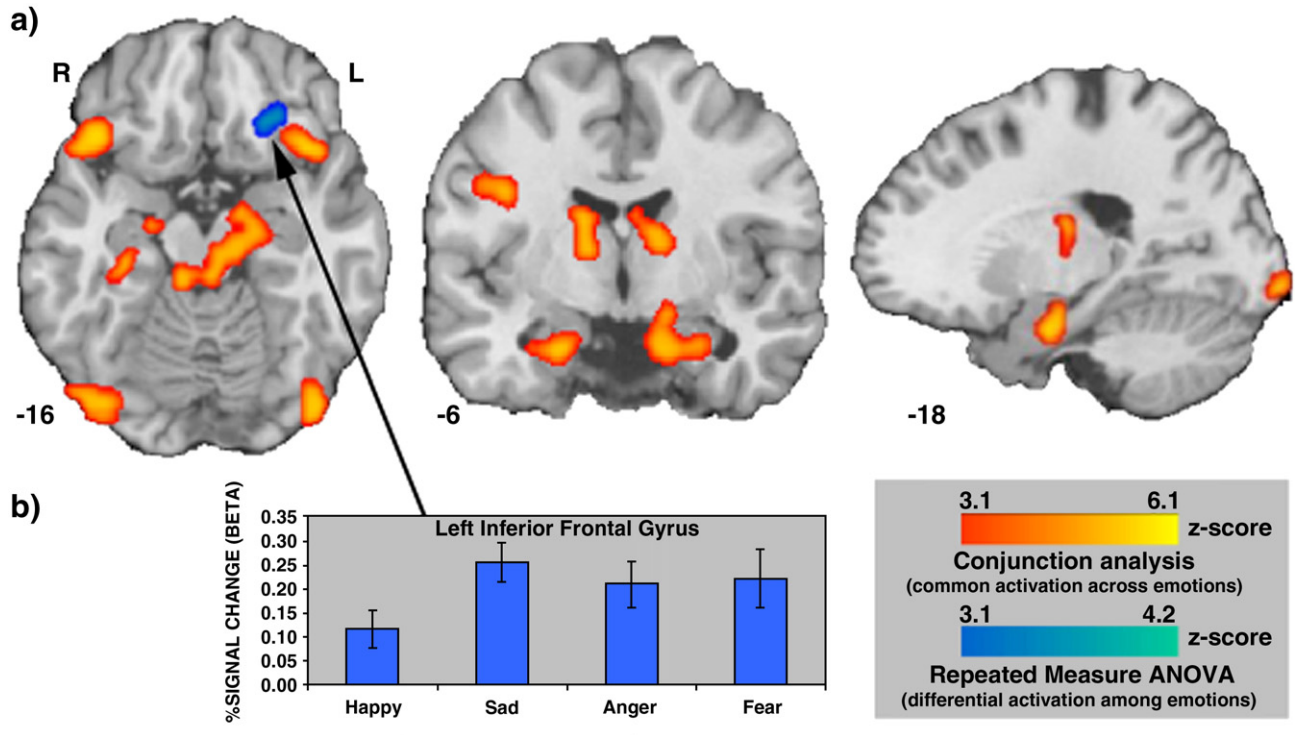

Fig. 1 – Block analysis results. a) Group analysis (N = 17) showing average brain activation for all target emotions (red scale) and target emotion sensitive activation in the inferior frontal gyrus (blue region). b) Mean percent signal change for inferior frontal gyrus by target emotion (blue scale). Images are displayed over a Talairach-normalized template in radiological convention.

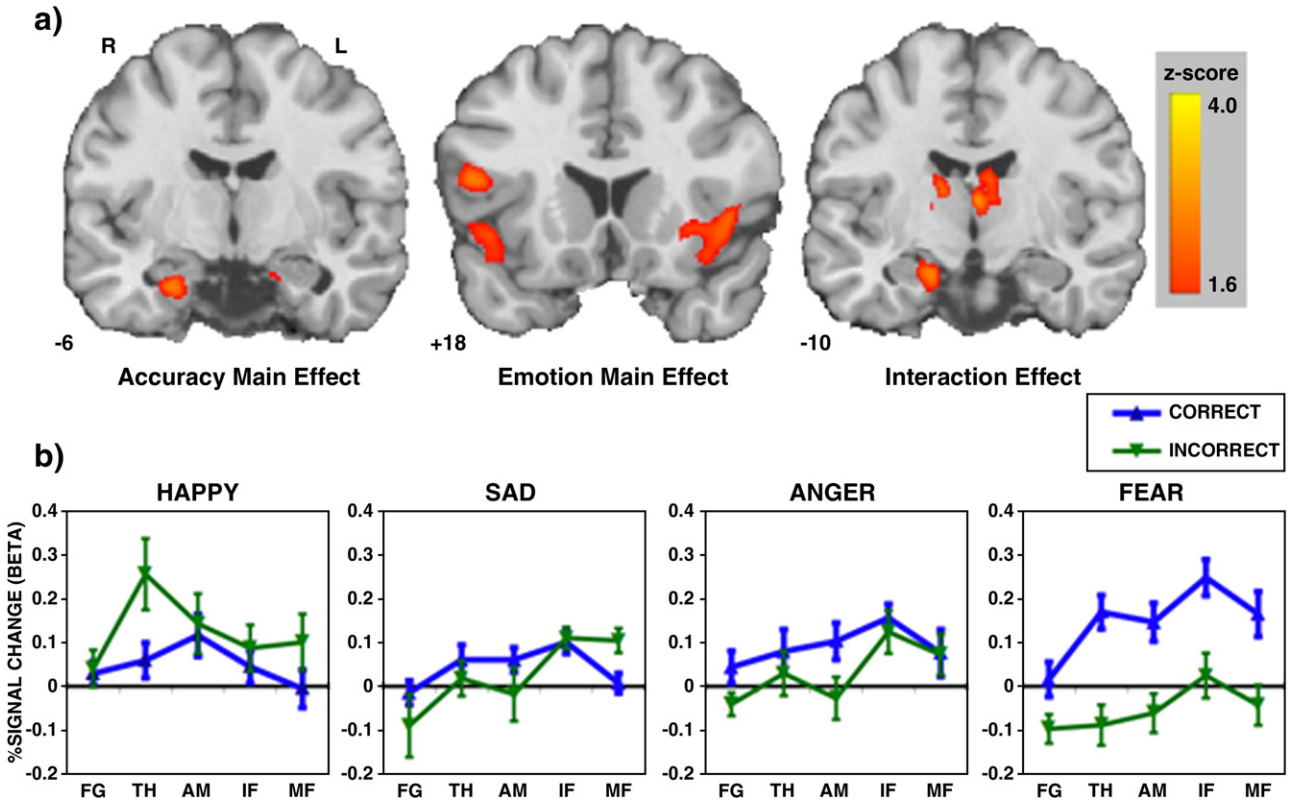

Fig. 2 – Event-related results. a) Emotion (Happy, Sad, Anger, Fear), Accuracy (Correct vs. Incorrect), and Interaction effects for whole brain repeated measure ANOVA highlighting mesial temporal lobe regions. b) Mean percent signal change for regions showing main or interaction effects (error bars represent S.E.M.). Images are displayed over a Talairach-normalized template in radiological convention, masked by block activation and thresholded $p = 0.05$.

4.2. *Task*

The face emotion identification experiment included four time series, each with a specific target emotion: happiness, sadness, anger, or fear. For each time series a total of 32 target, 48 foil, and 40 neutral faces (Gur et al., 2002a,b) were shown (3 sec exposure) and subjects endorsed "target" or "other/neutral" with a two-button response pad. Four 90-s blocks of emotion identification were separated by 24 s of rest during which a degraded face with fixation point was displayed. Within each block, target faces (e.g. Angry) and foil faces (e.g. Happy, Sad, or Fear) were separated by a variable number of neutral faces (range 0–5 faces), allowing for event-related modeling with neutral faces as baseline. This inter-block design also allowed modeling of events based on accurate target identification. Abbreviated response instructions remained visible throughout the task.

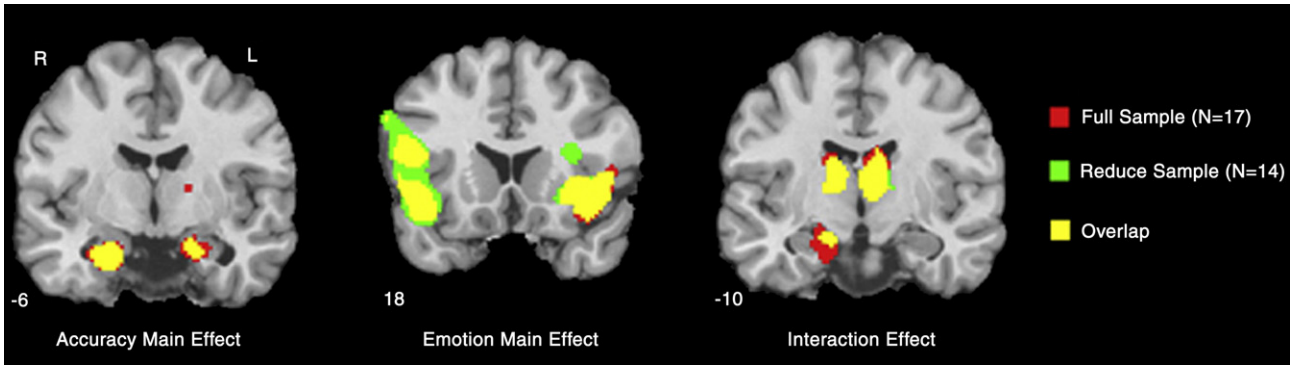

Fig. 3 – Event-related results: Reduced sample. Emotion (Happy, Sad, Anger, Fear), Accuracy (Correct vs. Incorrect), and Interaction effects for whole brain repeated measure ANOVA showing subset ($n = 14$) of sample in green and full sample ($N = 17$) in red. Colored regions represent voxels $p = 0.05$. Images are masked by block activation and displayed over a Talairach-normalized template in radiological convention.

4.3. *fMRI procedures*

Participants were administered a brief practice task before placement in the scanner. Earplugs were fitted to muffle noise and head fixation was assured through a foam–rubber device mounted on the head coil. Stimuli presentation was triggered by the scanner and synchronized with image acquisition using PowerLaboratory (MacLaboratory, Inc., Devon, PA). Stimuli were rear-projected to the center of the visual field using a PowerLite 7300 video projector (Epson America, Inc., Long Beach, CA) and viewed through a head coil mounted mirror. Subjects were randomly assigned use of their dominant or non-dominant hand and responses were recorded via a non-ferromagnetic keypad (FORP™; Current Design Inc., Philadelphia, PA).

4.4. *Image acquisition*

Data were acquired on a 4T GE Signa Scanner (Milwaukee, WI), with a quadrature head coil. Structural images consisted of a sagittal T1-weighted localizer, followed by a T1-weighted acquisition of the entire brain in the axial plane (24 cm FOV, 256×256 matrix, resulting in voxel size of (0.9375×0.9375×4 mm). This sequence was used for spatial normalization to a standard atlas (Talairach and Tournoux, 1998) and for anatomic overlays of the functional data. Functional imaging was performed in the axial plane using a 16-slice, single-shot gradient-echo (GE) echo-planar (EPI) sequence (TR/TE=1500/21 ms, FOV=240 mm, matrix=64×40, slice thickness/gap=5/0 mm). This sequence delivered a nominal voxel resolution of 3.75×3.75×5 mm. The slices were acquired from the superior cerebellum up through the frontal lobe. Inferiorly this corresponded to a level just below the inferior aspect of the temporal lobes and superiorly to approximately the level of the hand-motor area in the primary motor cortex. An automated shimming was performed in a region of interest containing the anterior medial temporal lobe (Webb and Macovski, 1991). After the shimming, pilot echoplanar images were obtained, which were visually inspected before time-series acquisition to insure good image quality in the amygdala region. The images were also corrected for residual geometric distortion (Jezzard and Balaban, 1995) based on a magnetic field map acquired with a one-minute reference scan.

4.5. *Performance analysis*

Percent correct and median reaction time (RT; in milliseconds) were calculated for each stimulus class. Differences in percent correct and reaction time among the four classes were evaluated using separate repeated measures ANOVAs. To satisfy the normality assumptions of ANOVA, the arcsine transformation was applied to the percentages.

4.6. *Image analysis*

fMRI data were preprocessed and analyzed using FEAT (fMRI Expert Analysis Tool) Version 5.1, part of FSL (FMRIB's Software Library, www.fmrib.ox.ac.uk/fsl). Images were slice time-corrected using Fourier-space time-series phase-shifting, motion corrected to the median image using tri-linear interpolation with six degrees of freedom (Jenkinson et al., 2002), high pass filtered (120 s), spatially smoothed (8 mm FWHM, isotropic) and scaled using mean-based intensity normalization. The median functional and anatomical volumes were coregistered, then transformed into the standard anatomical space (T1 MNI template) using the tri-linear interpolation (Jenkinson et al., 2002). BET (Smith, 2002) was used to remove non-brain areas.

Subject-level time-series statistical analysis was carried out using FILM (FMRIB's Improved Linear Model) with local autocorrelation correction (Woolrich et al., 2001). Each time series (i.e. Happy, Sad, Anger, Fear) was regressed to a canonical hemodynamic response function modeling emotion discrimination blocks relative to crosshair. These data were submitted to two group level analyses: 1) each subject's mean activation across the four target conditions was calculated and entered into a single group *t*-test; 2) to identify regions differentially activated by Happy, Sad, Anger, or Fear target conditions, the individual subject's beta weights for the four emotions were entered into a voxelwise repeated measures ANOVA. *Z* (Gaussianised *F*) statistic images were corrected for spatial extent using Monte Carlo simulation (AFNI AlphaSim, R. W. Cox, National Institute of Health) with a minimum z threshold =3.1 and cluster probability of $p=0.05$. Further investigation was restricted to regions significantly activated in the block group analyses.

The event-related subject-level analysis modeled four performance-based regressors (correct target, incorrect target, correct foil, incorrect foil) with neutral faces serving as baseline. Individual subject beta weights for correct target and incorrect target were entered into an accuracy (Correct, Incorrect) by emotion (Happy, Sad, Anger, Fear) voxelwise repeated measures ANOVA. Mean scaled beta coefficients (% signal change) for clusters greater than 20 contiguous voxels and z-score =1.64 were extracted for off line analysis and graphic presentation.

Acknowledgments

Supported by grants from the National Institute of Mental Health (MH 60722 and MH 19112). We thank the Center for Functional Neuroimaging (CfN) and the staff of the MRI facility for their help, Avis Brennan for assistance in data collection, and Ramapriyan Pratiwadi for image processing.

REFERENCES

Adolphs, R., Gosselin, F., Buchanan, T.W., Tranel, D., Schyns, P., Damasio, A.R., 2005. A mechanism for impaired fear recognition after amygdala damage. Nature 433 (7021), 68–72.

Baas, D., Aleman, A., Kahn, R.S., 2004. Lateralization of amygdala activation: a systematic review of functional neuroimaging studies. Brain Res. Brain Res. Rev. 45 (2), 96–103.

Britton, J.C., Taylor, S.F., Sudheimer, K.D., Liberzon, I., 2006. Facial expressions and complex IAPS pictures: common and differential networks. NeuroImage 31 (2), 906–919.

Buchel, C., Morris, J., Dolan, R.J., Friston, K.J., 1998. Brain systems mediating aversive conditioning: an event-related fMRI study. Neuron 20 (5), 947–957.

Damasio, A.R., 1997. Neuropsychology. Towards a neuropathology of emotion and mood. Nature 386 (6627), 769–770.

Darwin, C., 1872. The Expression of Emotion in Man and in Animals. London, England.

Fitzgerald, D.A., Angstadt, M., Jelsone, L.M., Nathan, P.J., Phan, K.L., 2006. Beyond threat: amygdala reactivity across multiple expressions of facial affect. NeuroImage 30 (4), 1441–1448.

Gur, R.C., Sara, R., Hagendoorn, M., Marom, O., Hughett, P., Macy, L., et al., 2002a. A method for obtaining 3-dimensional facial expressions and its standardization for use in neurocognitive studies. J. Neurosci. Methods 115 (2), 137–143.

Gur, R.C., Schroeder, L., Turner, T., McGrath, C., Chan, R.M., Turetsky, B.I., et al., 2002b. Brain activation during facial emotion processing. NeuroImage 16 (3 Pt 1), 651–662.

Hariri, A.R., Mattay, V.S., Tessitore, A., Fera, F., Weinberger, D.R., 2003. Neocortical modulation of the amygdala response to fearful stimuli. Biol. Psychiatry 53 (6), 494–501.

Jenkinson, M., Bannister, P., Brady, M., Smith, S., 2002. Improved optimization for the robust and accurate linear registration and motion correction of brain images. NeuroImage 17 (2), 825–841.

Jezzard, P., Balaban, R.S., 1995. Correction for geometric distortion in echo planar images from B0 field variations. Magn. Reson. Med. 34 (1), 65–73.

Knight, D.C., Smith, C.N., Stein, E.A., Helmstetter, F.J., 1999. Functional MRI of human Pavlovian fear conditioning: patterns of activation as a function of learning. NeuroReport 10 (17), 3665–3670.

LaBar, K.S., Gatenby, J.C., Gore, J.C., LeDoux, J.E., Phelps, E.A., 1998. Human amygdala activation during conditioned fear acquisition and extinction: a mixed-trial fMRI study. Neuron 20 (5), 937–945.

LeDoux, J., 2000. Emotion circuits in the brain. Annu. Rev. Neurosci. 23, 155–184.

LeDoux, J., 2003. The emotional brain, fear, and the amygdala Cell. Mol. Neurobiol. 23 (4–5), 727–738.

Morris, J.S., Dolan, R.J., 2004. Dissociable amygdala and orbitofrontal responses during reversal fear conditioning. NeuroImage 22 (1), 372–380.

Morris, J.S., Frith, C.D., Perrett, D.I., Rowland, D., Young, A.W., Calder, A.J., et al., 1996. A differential neural response in the human amygdala to fearful and happy facial expressions. Nature 383 (6603), 812–815.

Morris, J.S., Friston, K.J., Buchel, C., Frith, C.D., Young, A.W., Calder, A.J., et al., 1998. A neuromodulatory role for the human amygdala in processing emotional facial expressions. Brain 121 (Pt 1), 47–57.

Murphy, F.C., Nimmo-Smith, I., Lawrence, A.D., 2003. Functional neuroanatomy of emotions: a meta-analysis. Cogn. Affect. Behav. Neurosci. 3 (3), 207–233.

Phan, K.L., Wager, T., Taylor, S.F., Liberzon, I., 2002. Functional neuroanatomy of emotion: a meta-analysis of emotion activation studies in PET and fMRI. NeuroImage 16 (2), 331–348.

Phelps, E.A., 2004. Human emotion and memory: interactions of the amygdala and hippocampal complex. Curr. Opin. Neurobiol. 14 (2), 198–202.

Phelps, E.A., Delgado, M.R., Nearing, K.I., LeDoux, J.E., 2004. Extinction learning in humans: role of the amygdala and vmPFC. Neuron 43 (6), 897–905.

Phillips, M.L., Young, A.W., Senior, C., Brammer, M., Andrew, C., Calder, A.J., et al., 1997. A specific neural substrate for perceiving facial expressions of disgust. Nature 389 (6650), 495–498.

Schneider, F., Grodd, W., Weiss, U., Klose, U., Mayer, K.R., Nagele, T., et al., 1997. Functional MRI reveals left amygdala activation during emotion. Psychiatry Res. 76 (2–3), 75–82.

Smith, S.M., 2002. Fast robust automated brain extraction. Hum. Brain Mapp. 17 (3), 143–155.

Talairach, J., Tournoux, P., 1998. Co-Planar Stereotaxic Atlas of the Human Brain. Thieme Medical Publishers, New York, NY.

Vuilleumier, P., 2005. Cognitive science: staring fear in the face. Nature 433 (7021), 22–23.

Vuilleumier, P., Armony, J.L., Driver, J., Dolan, R.J., 2003. Distinct spatial frequency sensitivities for processing faces and emotional expressions. Nat. Neurosci. 6 (6), 624–631.

Webb, P., Macovski, A., 1991. Rapid, fully automatic, arbitrary-volume in vivo shimming. Magn. Reson. Med. 20 (1), 113–122.

Whalen, P.J., Kagan, J., Cook, R.G., Davis, F.C., Kim, H., Polis, S., et al., 2004. Human amygdala responsivity to masked fearful eye whites. Science 306 (5704), 2061.

Whalen, P.J., Shin, L.M., McInerney, S.C., Fischer, H., Wright, C.I., Rauch, S.L., 2001. A functional MRI study of human amygdala responses to facial expressions of fear versus anger. Emotion 1 (1), 70–83.

Woolrich, M.W., Ripley, B.D., Brady, M., Smith, S.M., 2001. Temporal autocorrelation in univariate linear modeling of FMRI data. NeuroImage 14 (6), 1370–1386.